A machine learning approach for ozone forecasting and its application for Kennewick, WA

Kai Fan[1], Brian Lamb[1], Ranil Dhammapala[2], Ryan Lamastro[3], Yunha Lee[1]*

[1]Laboratory for Atmospheric Research, Civil and Environmental Engineering, Washington State University

[2]Washington State Department of Ecology

[3]State University of New York at New Paltz

*Corresponding Author

E-mail: yunha.lee@wsu.edu (Yunha Lee)

ABSTRACT:

Chemical transport models (CTM) are widely used for air quality modeling, but these models miss forecasting some air pollution events, and require a lot of computational power. In Kennewick, WA, elevated O_3 episodes can occur during the summer and early fall, but the CTM-based operational forecasting system (AIRPACT) struggles to capture them. This research used the 2015 – 2018 historical archives from the Weather Research and Forecasting (WRF) meteorological model forecasts produced daily by the University of Washington, and O_3 observation data at

Kennewick to train two machine learning modeling frameworks, ML1 and ML2 for a reliable forecasting system. ML1 used the random forest (RF) classifier and multiple linear regression (MLR) models, and ML2 used a two-phase RF regression model with best-fit weighting factors. Since April 2019, the ML modeling frameworks have been used to produce daily 72-hour O_3 forecasts and have provided the forecasts via the web for the agency and public use. For the peak O_3 days, AIRPACT showed a large variation, while ML2 underpredicted and ML1 performed the best. In the future, this ML forecast system will be applied to other locations within the Pacific Northwest.

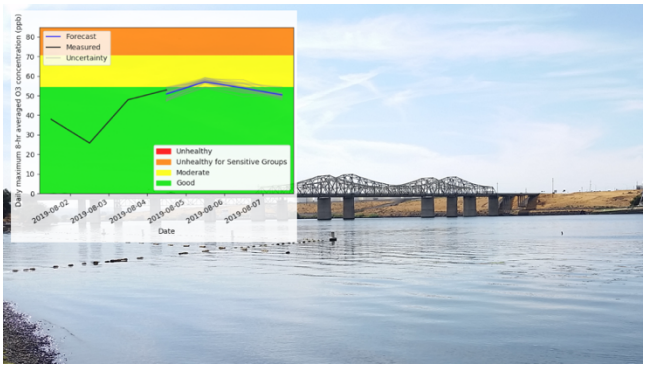

1. INTRODUCTION

Chemical transport models (CTM) are widely used to simulate the temporal and spatial variation of air quality.[1] CTMs include various atmospheric physical and chemical processes as well as sources and sinks. However, not every physical and chemical process in the atmosphere has been understood.[2] Even though the accuracy of numerical models keeps improving, there are still large uncertainties and errors in the simulations. For the CTMs, the high computational cost is an additional concern.

The Air Indicator Report for Public Awareness and Community Tracking (AIRPACT) was developed for air quality forecasting in the Pacific Northwest in the U.S. AIRPACT uses the Community Multiscale Air Quality Modeling System (CMAQ) model to compute air quality with the Weather Research and Forecasting (WRF) meteorology. The AIRPACT domain mainly covers Washington, Idaho and Oregon State with 4 km horizontal grid cells and 37 vertical levels. The hourly simulations use the Carbon Bond, version 5 (CB05) as the gas chemistry mechanism and AERO6 as the aerosol module. AIRPACT 48-hour forecasts are produced daily and provided via the web to the public and local air quality agencies (http://lar.wsu.edu/airpact/).

Within the AIRPACT domain, Kennewick is part of the Tri-cities metropolitan area with a total population of about 216,000 (Estimated population of Kennewick 83,670, Pasco 75,290 and Richland 56,850 in 2019).[3] The city is 32 km north of Washington State's southern border and is in a hot dry portion of the state. Recent monitoring and a large field study have shown that a few high O_3 events typically occur during summer and early fall.[4] While AIRPACT forecasts initially predicted the Tri-cities area as an ozone hotspot, the daily forecasts struggle to forecast correctly high O_3 concentrations in this area. There were 20 days when the air quality was unhealthy for sensitive groups in 2015 – 2018, but AIPRACT only captured one of them.

Machine learning models have been used to predict air quality in recent years. These methods incorporate a variety of features, including observed pollutant levels and various meteorological variables as the basis for training and applying ML methods. For example, Feng et al.[5] input trajectory-based geographic parameters, meteorological forecasts and associated pollutant predictors to an artificial neural network to predict PM2.5 concentrations in Beijing, China. Freeman et al.[6] used a recurrent neural network with short-term memory to predict 72-hour O_3 forecasting with training via hourly air quality and meteorological data. Zamani Joharestani et al.[7]

tested three machine learning approaches, random forest, extreme gradient boosting and deep learning to predict the PM2.5 concentrations in Tehran, Iran using 23 features.

A successful machine learning model must be trained with a big dataset. For air quality prediction, the training dataset usually includes meteorological data (temperature, relative humidity, pressure, wind speed and direction, etc.) and observed pollutant concentrations. However, compared to numerical models, it tends to be more computationally efficient, requires less input data, and performs better for specific events, which makes the machine learning models popular in recent years.[5,6,8–10]

In this study, we developed machine learning modeling frameworks to predict O_3 mixing ratios, which were based on the following approaches: random forest (RF) and multiple linear regression (MLR). RF is one of the most popular machine learning methods and has been used in many air quality modeling and forecast studies. The RF method has been demonstrated to provide reliable forecasts for O_3 and PM2.5 with lower computational cost compared to physical models.[11–14] RF consists of an ensemble of decision trees, and decision tree learning is for approximating discrete-valued functions.[15–17] The RF model can be used for classification and regression. For our study, the RF classifier model was used to predict the O_3 Air Quality Index (AQI) categories, and the RF regression model was used to predict O_3 mixing ratios. MLR is a regression method with one dependent variable and several independent variables, which we used to predict O_3 levels. Previous studies that used MLR models to predict O_3 mixing ratios showed performance as good as more complex machine learning models.[18–21] Yuchi et al.[22] used RF and MLR for indoor air quality forecasts, and RF showed better in-sample predictions, MLR showed better out-of-sample predictions. So, this paper will discuss the application of both RF and MLR for O_3 forecasts.

79 The goal of this study is to provide reliable air quality forecasts using machine learning
80 approaches, especially for high O_3 events in Kennewick, WA. Section 2 presents the two machine
81 learning modeling frameworks we developed, including the training dataset. Section 3 presents the
82 feature selection, evaluation of the model performance using 10-time 10-fold/walk-forward cross-
83 validation and a summary of the forecast results in 2019.
84

85 # 2. DATASETS AND MODELING FRAMEWORKS

86 ## 2.1. Training dataset.

87 The training dataset for our machine learning models includes the previous day's observed O_3
88 mixing ratios, time information (hour, weekday, month), and simulated meteorology from daily
89 WRF forecasts from May to September in 2015 – 2018 at Kennewick, WA. Because the heat and
90 sunlight favor the O_3 generation,[23] and wildfires can generate the O_3 precursors,[24] observations are
91 only made from May to September. The training dataset covered this period. The WRF
92 meteorology was obtained from the University of Washington,[25,26] which is used in AIRPACT as
93 an input to generate emissions and air quality forecasting. We used the temperature, surface
94 pressure, relative humidity, wind speed, wind direction, and planetary boundary layer height (PBL)
95 in the training dataset. Time information was included in the training dataset due to the significant
96 trend of O_3 variation in the diurnal, weekday and monthly scales. Table S1 summarizes the
97 historical O_3 AQI during the training period. Here we define a high O_3 day as the day when the
98 observed AQI category is worse than Moderate (i.e. AQI category 3 or worse). The high O_3 days
99 in all the years used here are less than 5% of total simulated days, except for 2017. Extensive
100 wildfires occurred in 2017, and there were 8 days that the air quality was unhealthy for sensitive

groups (i.e., O_3 AQI category = 3). The days when the wildfire smoke caused excess O_3 were marked in the historical data, but it could not be involved in the training dataset because it was not predictable. And there were only four days in this case, so it would not affect the model training significantly.

2.2. Machine learning modeling frameworks

We have developed two O_3 forecast modeling frameworks based on machine learning frameworks. The first machine learning modeling framework (ML1, hereafter; see Figure 1A) used RF classifier and MLR models. The *RandomForestClassifier* and *RFE* functions in the python module *sklearn* were used. In ML1, the WRF meteorology, time information, and previous day's 8-hour averaged O_3 mixing ratios were first used to train an RF classifier model to predict AQI categories. There are not many high O_3 cases, which makes the dataset imbalanced, and the imbalanced training data may lead the bias toward the low O_3 prediction.[27] To address the problem from the imbalanced data, the *balanced_subsample* option was turned on for the RF classifier. The *balanced_subsample* gives weights to the AQI category values based on their frequency in the bootstrap sample for each tree, so the high AQI values with low frequency in the training dataset are weighted proportionally more. Separately, the observed AQI categories were added to the training dataset to train the MLR model. When used for forecasting, the RF classifier model was first used to predict the AQI categories, which were in turn fed into the MLR model to predict the O3 mixing ratios, as the red dashed line shown in Figure 1A.

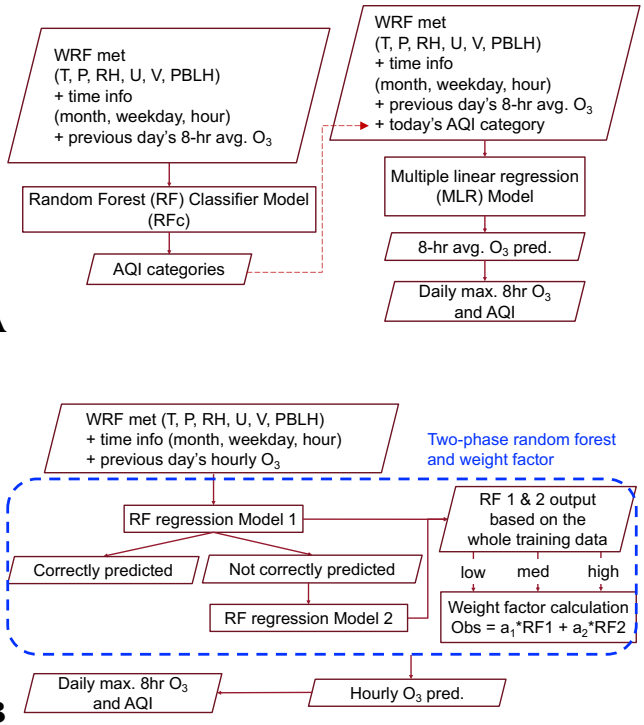

Figure 1. (A) ML1 modeling framework based on random forest (RF) classifier and multiple linear regression (MLR) models (B) ML2 based on a two-phase RF regression and weight factors

Machine Learning modeling framework 2 (ML2 hereafter; see Figure 1B) is based on a two-phase random forest regression model. The *RandomForestRegressor* function in the python module *sklearn* was used. ML2 used the WRF meteorology, time information, and previous day's hourly O_3 mixing ratios to train an RF regression model to predict O_3 mixing ratios. The whole historical dataset was used to train the first RF regression model (RF1 in Figure 1B). The training data was isolated when RF1 predicted O_3 mixing ratios differed from the observations by more than 5 ppb, and then the isolated dataset was used to train the second RF regression model (RF2 in Figure 1B). The training dataset for RF2 was a subset of the whole training data, so RF2 required more decision trees (100 trees for RF1 and 200 trees for RF2).[28] This is why it is called a two-

phase RF regression model. The RF1 predicted O_3 mixing ratios were divided into three levels (low: < 30 ppb, medium: 30 – 50 ppb, high: > 50 ppb). For the data within each level, a set of weighting factors, a_1 and a_2, were computed based on a linear regression equation,

$$O_{3observed} = a_1*RF_1 + a_2*RF_2 \quad (1)$$

When doing forecasting, RF1 and RF2 were used to provide initial predictions. The RF1 prediction determined which weighting factors would be used. The hourly O_3 prediction was computed as

$$O_3 = a_1*RF_1 + a_2*RF_2 \quad (2)$$

2.3. Ensemble forecasting system

The ML1 and ML2 modeling frameworks have been used to provide 72-hour "ensemble" operational O_3 forecasts each day, by using more than 20 members from the University of Washington Mesoscale Ensemble system (https://a.atmos.washington.edu/wrfrt/ensembles/info.html) beginning in April 2019. We predicted the O_3 levels with each WRF member to compile a 72-hour ensemble mean forecast with an associated uncertainty range. The forecasts are available to the public on http://ozonematters.com, with the ability to sign up for email alerts if "Unhealthy for Sensitive Groups" or worse levels are forecast. To increase the size of the training dataset and improve the forecast accuracy, we included the new observational data from the previous day and re-trained the models daily. For the ensemble daily forecasts, the computational time is approximately 1 min for ML1 and less than 3 min for ML2.

2.4. Statistical methods for O_3 AQI evaluation

Two parameters, Heidke Skill Score (HSS) and the Hanssen-Kuiper Skill Score (KSS) were used to evaluate the machine learning model prediction. Table S2 is a 2x2 contingency table, which shows the simple yes or no case.[29] For the air quality researches, "yes" usually means air pollution events, and "no" means good air quality. The equations (3) and (4) show how HSS and KSS are computed.[30]

$$HSS = \frac{a + d - a_r - d_r}{n - a_r - d_r} \qquad (3)$$

Where $a_r = \frac{(a+b)(a+c)}{n}$, $d_r = \frac{(b+d)(c+d)}{n}$

$$KSS = \frac{ad - bc}{(b + d)(a + c)} \qquad (4)$$

HSS represents the accuracy of the model prediction compared with a reference forecast (r in equation 3), which is from the random guess that is statistically independent of the observations.[30,31] The range of the HSS is from -∞ to 1. A negative value means a random guess is better, 0 means no skill, and 1 means a perfect score. KSS measures the ability to separate different categories. The range is from -1 to 1 where 0 means no skill, and 1 means a perfect score.

For the multi-category case in this research with AQI 1 (Good), 2 (Moderate) or 3 (Unhealthy for Sensitive Groups), we use the 3x3 contingency table in Table S3 [32]. The skill scores are computed as follows.[30]

$$HSS = \left(\sum_{i=1}^{3} p_{ii} - \sum_{i=1}^{3} p_i \hat{p}_i\right) / \left((1 - \sum_{i=1}^{3} p_i \hat{p}_i)\right) \qquad (5)$$

$$KSS = \left(\sum_{i=1}^{3} p_{ii} - \sum_{i=1}^{3} p_i \hat{p}_i\right) / \left((1 - \sum_{i=1}^{3} p_i p_i)\right) \qquad (6)$$

175 The p_{ii} is the sample frequency when the observed and model predicted AQI is i, and p_i and $\hat{p}_i$
176 are the observed and model predicted sample frequency when AQI = i. The multi-category case is
177 based on the simple yes or no case, and the skill scores, HSS and KSS have the same meaning as
178 the simple case.
179

180 # 3. RESULTS AND DISCUSSION

181 ## 3.1. Feature selection for machine learning models

182 There were 10 features for the RF classifier and regression model and 11 features for the MLR
183 model. Too many features can cause an overfitting problem,[33] so the attributes
184 *feature_importances_* in function *RandomForestClassifier/RandomForestRegressor* and *ranking_*
185 in *RFE* were used to do the feature selection. The selected features were input to train the model.

186 There were two components in ML1, RF classifier and MLR model. For an RF model, the feature
187 selection function with the default setting computed the importance weights, and the features
188 whose weight was above the mean weight were selected. The feature weights could change in each
189 training process, but the ranking showed very little variation. The previous day O_3 observation,
190 temperature and hour were the primary features selected, and the relative humidity was selected in
191 some cases. The default number of selected features for MLR was half of the total features
192 available, so two more features were chosen by the built-in feature selection function, in addition
193 to the three primary features: the previous day O_3 observation, temperature, relative humidity, AQI
194 category, and surface pressure. The output of each framework was hourly O_3 mixing ratios for

each 72-hour forecast. For evaluation purposes, these forecast values were compiled into the maximum daily 8-hour moving average O_3 (MDA8).

The feature selection function for RF regression was the same as the RF classifier model. Temperature, previous O_3 observation, PBL height or relative humidity, were the selected features for the first phase RF regression model, and the temperature and hour were selected for the second phase.

3.2. Machine learning model evaluation

Cross-validation is commonly used for the model evaluation, and it can test the subset of the dataset with an equal chance.[34] There are various cross-validation methods, such as leave-one-out, k-fold, etc. Here, the 10-time 10-fold and walk-forward cross-validation were used to evaluate the two modeling frameworks. The input data were the primary WRF output, time information and historical O_3 observations in Kennewick.

3.2.1 10-time 10-fold cross-validation

The k-fold cross-validation may be the most commonly used technique for the model evaluation.[34] It divides the dataset into k randomly chosen parts (k=10 in this research), and k-1 parts are used to train the model, the remaining portion is used to test the model, and this process is repeated k times to test all k subsets. The *RepeatedKFold* function in the python module *sklearn* was used to separate the dataset. To avoid any bias from data separation, the k-fold cross-validation was repeated 10 times in this research.

The NMB for these 10-time cross-validation was 6.3% ± 0.2% for ML1 and 0 ± 0.1% for ML2. The AIRPACT NMB was -9.3%, which was lower than ML1 and ML2. The standard deviations show that there is no significant difference among each repeat, and the model performance is stable.

The Q-Q plots in Figure 2A show the comparison between the model predictions and observations. AIRPACT underpredicted the MDA8 for MDA8 lower than 70 ppb. For MDA8 higher than 70 ppb, AIRPACT tended to predict the DMA8 close to the 1:1 line, but there were several extremely high predictions from AIRPACT which were not shown in Figure 2A. ML1 and ML2 were close to the 1:1 line when the MDA8 was lower than 45 ppb. ML1 was close to the 1:1 line for MDA8 in the 60 – 70 ppb range. For high MDA8 cases (> 70 ppb), ML1 showed the best performance.

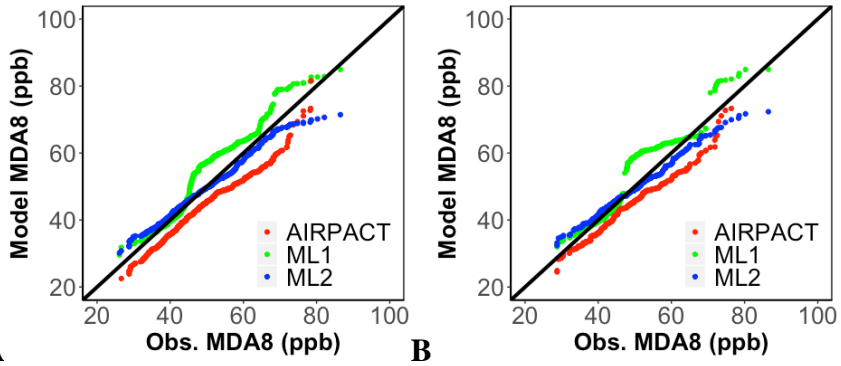

Figure 2. Q-Q plots of averaged model vs. observed MDA8 (A) during May – September 2015 – 2018 based on the 10 times 10-fold cross-validation (B) during May – September 2017 – 2018 based on the walk-forward cross-validation

The highest 10 observed MDA8 during 2015 – 2018 and their model predictions were selected and shown in Figure 2B. ML2 and AIRPACT underpredicted all 10 cases, and ML1 provided

close predictions for 7 out of 10. These results show that ML1 performs better for high O_3 events, and results from the Q-Q plot also confirms this. The two ML models showed a similar trend, and they both largely underpredicted 3 cases. So, they may miss the same factor which led to the high MDA8. The highest O_3 day was affected by the wildfire smoke, and all models missed it.

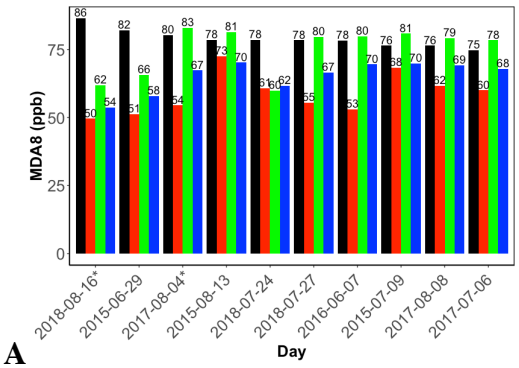

A

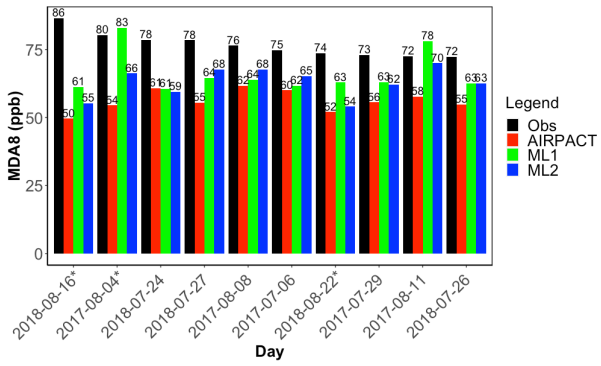

B

Figure 3. Top 10 observed MDA8 and model predictions from (A) 10-time 10-fold cross-validation (B) the walk-forward cross-validation

* means that the wildfire smoke caused excess ozone on that day

3.2.2 Walk-forward cross-validation

The 10-time 10-fold cross-validation does not consider the temporal order of the data, which is important for the time-series data. Walk-forward cross-validation is a technique for time-series data.[35] For this evaluation, the 2015 and 2016 data were used to train the model and predict the first day in the 2017 dataset (May 1st, 2017). Then the May 1st, 2017 data was included in the training dataset and the models were used to predict O_3 for May 2nd, 2017. This process was repeated for each additional day of the 2017 and 2018 ozone seasons.

When a new day's MDA8 was predicted by the ML models, the NMB was recomputed by including the new prediction. The change of NMB was shown in Figure 3A. In the beginning, there was no clear trend for the NMB values for both ML models. The NMB from ML1 prediction sharply increased after June 2017 (Day 50 in Figure 3A) when more high O3 events occurred, slowly increased after August 2017 (Day 100 in Figure 3A), and slowly decreased after July 2018 (Day 200 in Figure 3A). The overprediction from ML1 during the low O3 periods (May and June) could lead to the NMB increasing, while the NMB values were stable or even decreasing during the high O3 period (July and August). For ML2, there were some fluctuations before August 2018, and the NMB was stable after that. For both ML1 and ML2, the NMB values were getting stable when more data got involved. The final NMB of two ML models were 5.6% and -0.9%, which were lower than the 10-time 10-fold cross-validation.

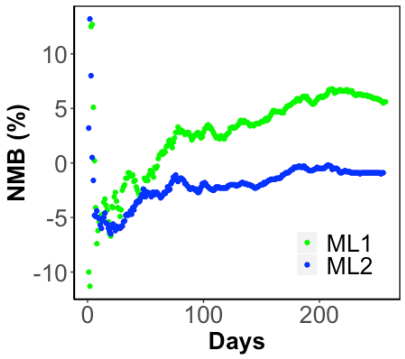

Figure 4. The walk-forward NMB of each time step for ML1 and ML2

The walk-forward cross-validation provided two-year MDA8 predictions (2017 and 2018), and the Q-Q plots were similar to the 10-time 10-fold cross-validation. The two breakpoints of ML1 distribution were clearer in Figure 3B. Ten highest MDA8 in 2017 and 2018 were shown in Figure 4. ML1 only captures 2 out of the top 10 observed MDA8 and ML2 captured 1. In some cases, ML1 was even lower than ML2. Three high O_3 days with stars (*) in Figure 4 were affected by the wildfire smoke, and ML1 captured two of them. The two ML models still performed better than AIRPACT.

Table 1 summarizes the HSS and KSS of the two machine learning models and AIRPACT from the two cross-validation methods. Both machine learning models show better performance with higher HSS and KSS values than AIRPACT. ML2 shows higher HSS than ML1 for both cross-validation results, which means ML2's prediction is generally more accurate. ML1 shows higher KSS in 10-time 10-fold cross-validation due to its better performance of high O_3 predictions. The statistics from AIRPACT and ML2 are close between two cross-validations, but HSS and KSS from walk-forward are lower than 10-time 10-fold cross-validation.

Table 1. HSS and KSS from two cross-validations

		AIRPACT	ML1	ML2
10-time 10-fold	HSS	0.32	0.44	0.55
	KSS	0.25	0.62	0.50
Walk-forward	HSS	0.34	0.37	0.57
	KSS	0.27	0.53	0.51

3.3. O_3 ensemble forecasting in 2019

Since April 2019, our machine learning models have been used for operational O_3 ensemble forecasting for Kennewick, WA. The ensemble forecasting was based on more than 20 WRF ensemble members provided by the University of Washington to predict the O_3 levels. The difference among the predicted MDA8 from the ensemble members was not significant (within 5%). To better compare with the evaluation in the previous section, this section only covers the data from May to September in 2019. The ML1 and ML2 results are the ensemble means of the MDA8 values from more than 20 ML forecasts. The Q-Q plot in Figure 5 shows that the ML1, ML2 and AIRPACT model forecasts are close for O_3 lower than 40 ppb. For the O_3 in 40 – 60 ppb, ML1 tends to overpredict, while AIRPACT and ML2 are closer to observations. When the O_3 mixing ratio is higher than 60 ppb, ML1 slightly overpredicts, ML2 underpredicts, and AIRPACT varies in cases. For the highest 5 MDA8 points in Figure 6, the observed values were 62 – 66 ppb, while ML1's predictions were closer to the observations than AIRPACT and ML2. AIRPACT showed larger variation (48 – 70 ppb) compared to two ML models.

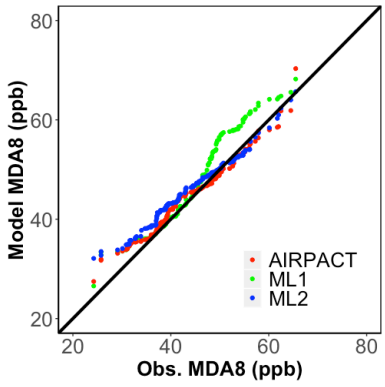

Figure 5. Q-Q plots of ensemble mean model vs. observed MDA8 during May - September 2019

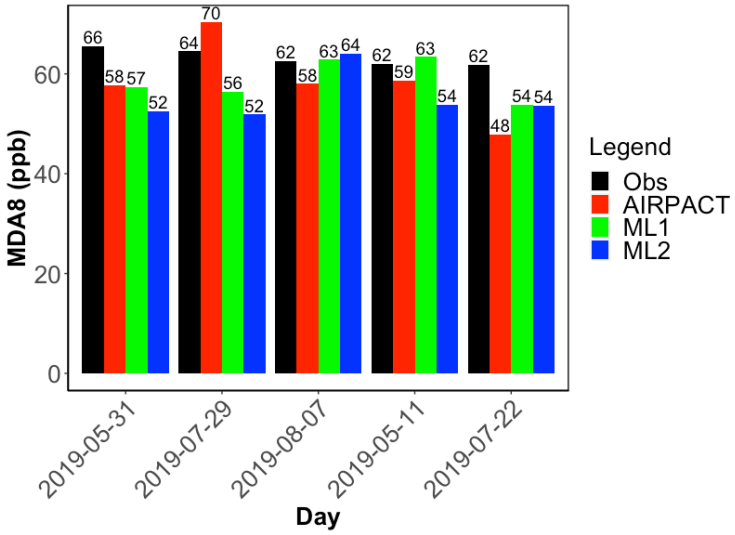

Figure 6. Top 5 observed MDA8 and model predictions in 2019

The scatter plots in Figure 7 show the ensemble mean MDA8 from May to September in 2019. ML2 shows relatively higher R^2 value (0.52) than ML1 (0.41) and AIRPACT (0.47). The NMB of AIRPACT is lowest (1.4%), but its NME (11.4%) is higher than ML2 (10.9%). The low NMB is due to the offset of overprediction and underprediction. ML1 tended to overpredict the MDA8 O_3 especially when it was higher than 40 ppb. Because of mostly favorable meteorological conditions and few wildfires in the Pacific Northwest, the O_3 mixing ratios were not very high in 2019 and the model performance of ML2 was the best.

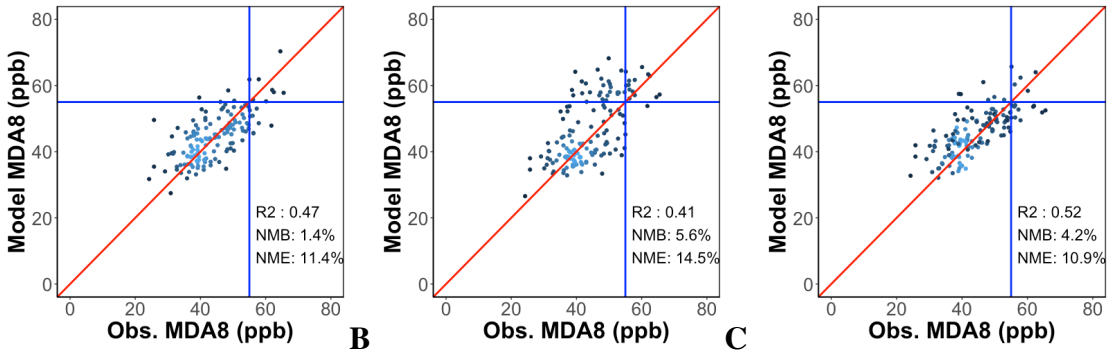

Figure 7. Scatter plots of observed vs. ensemble mean MDA8 of AIRPACT in (A), ML1 in (B) and ML2 in (C) at Kennewick from May to September in 2019

The model performance statistics are presented in Table 2, the blue cells show misses, and red cells show false alarms. In 2019, all the AQI_{obs} at Kennewick were less than 3. Compared to AIRPACT, ML1 captured high O_3 days better (15 events vs. 7 events for $AQI_{obs}2$) but tended to overpredict the O_3 AQI (26 false alarm events vs. 3 false alarm events). ML2 predicted similar AQI days to AIRPACT. Based on the analysis above, we decided to use ML1 to provide the daily forecasting for Kennewick when the predicted AQI was above 2, and ML2 when the predicted AQI was 1 or 2.

Table 2. Number of days for each AQI during May – September 2019

		Observation					
		AQI 1	AQI 2	AQI 1	AQI 2	AQI 1	AQI 2
AIRPACT	AQI 1	122	11	99	3	119	13
	AQI 2	3	7	26	15	6	5

ML1 and ML2 are the ensemble mean results using 20 WRF ensemble members.

The blue cells mean the model misses high O_3, and the red cells mean the model raises false alarms.

Acknowledgement

We thank the fund from CEE - YUNHA LEE ACCRUALS (2315-0028). We acknowledge that David Ovens from University of Washington helped setup a data feed of WRF ensembles.

Reference:

(1) Sportisse, B. A Review of Current Issues in Air Pollution Modeling and Simulation. *Computational Geosciences* **2007**, *11* (2), 159–181. https://doi.org/10.1007/s10596-006-9036-4.

(2) Seinfeld, J. H.; Pandis, S. N. *Atmospheric Chemistry and Physics: From Air Pollution to Climate Change*; John Wiley & Sons, 2016.

(3) April 1, 2019 Population of Cities, Towns and Counties Used for Allocation of Selected State Revenues State of Washington. Washington State Office of Financial Management 2019.

(4) B. T. Jobson; G. VanderSchelden. *The Tri-Cities Ozone Precursor Study (T-COPS)*; Final Report; Washington Department of Ecology, 2017.

(5) Feng, X.; Li, Q.; Zhu, Y.; Hou, J.; Jin, L.; Wang, J. Artificial Neural Networks Forecasting of PM2.5 Pollution Using Air Mass Trajectory Based Geographic Model and Wavelet Transformation. *Atmospheric Environment* **2015**, *107*, 118–128. https://doi.org/10.1016/j.atmosenv.2015.02.030.

(6) Freeman, B. S.; Taylor, G.; Gharabaghi, B.; Thé, J. Forecasting Air Quality Time Series Using Deep Learning. *Journal of the Air & Waste Management Association* **2018**, *68* (8), 866–886. https://doi.org/10.1080/10962247.2018.1459956.

(7) Zamani Joharestani, M.; Cao, C.; Ni, X.; Bashir, B.; Talebiesfandarani, S. PM2.5 Prediction Based on Random Forest, XGBoost, and Deep Learning Using Multisource Remote Sensing Data. *Atmosphere* **2019**, *10* (7), 373. https://doi.org/10.3390/atmos10070373.

(8) Delavar, M.; Gholami, A.; Shiran, G.; Rashidi, Y.; Nakhaeizadeh, G.; Fedra, K.; Hatefi Afshar, S. A Novel Method for Improving Air Pollution Prediction Based on Machine Learning Approaches: A Case Study Applied to the Capital City of Tehran. *ISPRS International Journal of Geo-Information* **2019**, *8* (2), 99. https://doi.org/10.3390/ijgi8020099.

(9) Watson, G. L.; Telesca, D.; Reid, C. E.; Pfister, G. G.; Jerrett, M. Machine Learning Models Accurately Predict Ozone Exposure during Wildfire Events. *Environmental Pollution* **2019**, *254*, 112792. https://doi.org/10.1016/j.envpol.2019.06.088.

(10) Zheng, Y.; Liu, F.; Hsieh, H.-P. U-Air: When Urban Air Quality Inference Meets Big Data. In *Proceedings of the 19th ACM SIGKDD international conference on Knowledge discovery and data mining - KDD '13*; ACM Press: Chicago, Illinois, USA, 2013; p 1436. https://doi.org/10.1145/2487575.2488188.

(11) Pernak, R.; Alvarado, M.; Lonsdale, C.; Mountain, M.; Hegarty, J.; Nehrkorn, T. Forecasting Surface O3 in Texas Urban Areas Using Random Forest and Generalized Additive Models. *Aerosol Air Qual. Res.* **2019**, *9* (12), 2815–2826. https://doi.org/10.4209/aaqr.2018.12.0464.

(12) Rybarczyk, Y.; Zalakeviciute, R. Machine Learning Approaches for Outdoor Air Quality Modelling: A Systematic Review. *Applied Sciences* **2018**, *8* (12), 2570. https://doi.org/10.3390/app8122570.

(13) Yu, R.; Yang, Y.; Yang, L.; Han, G.; Move, O. RAQ–A Random Forest Approach for Predicting Air Quality in Urban Sensing Systems. *Sensors* **2016**, *16* (1), 86. https://doi.org/10.3390/s16010086.

(14) Zhan, Y.; Luo, Y.; Deng, X.; Grieneisen, M. L.; Zhang, M.; Di, B. Spatiotemporal Prediction of Daily Ambient Ozone Levels across China Using Random Forest for Human Exposure Assessment. *Environmental Pollution* **2018**, *233*, 464–473. https://doi.org/10.1016/j.envpol.2017.10.029.

(15) Breiman, L. Random Forests. *Machine Learning* **2001**, *45* (1), 5–32. https://doi.org/10.1023/A:1010933404324.

(16) Kam, H. T. Random Decision Forest. In *Proceedings of the 3rd International Conference on Document Analysis and Recognition*; 1995; Vol. 1416, p 278282.

(17) Mitchell, T. M. *Machine Learning*; McGraw-Hill series in computer science; McGraw-Hill: New York, 1997.

(18) Arganis, M. L.; Val, R.; Dominguez, R.; Rodriguez, K.; Dolz, J.; Eato, J. M. Comparison Between Equations Obtained by Means of Multiple Linear Regression and Genetic Programming to Approach Measured Climatic Data in a River. In *Genetic Programming - New Approaches and Successful Applications*; Ventura Soto, S., Ed.; InTech, 2012. https://doi.org/10.5772/50556.

(19) Chaloulakou, A.; Assimacopoulos, D.; Lekkas, T. Forecasting Daily Maximum Ozone Concentrations in the Athens Basin. 16.

(20) Moustris, K. P.; Nastos, P. T.; Larissi, I. K.; Paliatsos, A. G. Application of Multiple Linear Regression Models and Artificial Neural Networks on the Surface Ozone Forecast in the Greater Athens Area, Greece. *Advances in Meteorology* **2012**, *2012*, 1–8. https://doi.org/10.1155/2012/894714.

(21) Sousa, S.; Martins, F.; Alvimferraz, M.; Pereira, M. Multiple Linear Regression and Artificial Neural Networks Based on Principal Components to Predict Ozone Concentrations. *Environmental Modelling & Software* **2007**, *22* (1), 97–103. https://doi.org/10.1016/j.envsoft.2005.12.002.

(22) Yuchi, W.; Gombojav, E.; Boldbaatar, B.; Galsuren, J.; Enkhmaa, S.; Beejin, B.; Naidan, G.; Ochir, C.; Legtseg, B.; Byambaa, T.; Barn, P.; Henderson, S. B.; Janes, C. R.; Lanphear, B. P.; McCandless, L. C.; Takaro, T. K.; Venners, S. A.; Webster, G. M.; Allen, R. W. Evaluation of Random Forest Regression and Multiple Linear Regression for Predicting Indoor Fine Particulate Matter Concentrations in a Highly Polluted City. *Environmental Pollution* **2019**, *245*, 746–753. https://doi.org/10.1016/j.envpol.2018.11.034.

(23) Weaver, C. P.; Liang, X.-Z.; Zhu, J.; Adams, P. J.; Amar, P.; Avise, J.; Caughey, M.; Chen, J.; Cohen, R. C.; Cooter, E.; Dawson, J. P.; Gilliam, R.; Gilliland, A.; Goldstein, A. H.; Grambsch, A.; Grano, D.; Guenther, A.; Gustafson, W. I.; Harley, R. A.; He, S.; Hemming, B.; Hogrefe, C.; Huang, H.-C.; Hunt, S. W.; Jacob, D. J.; Kinney, P. L.; Kunkel, K.; Lamarque, J.-F.; Lamb, B.; Larkin, N. K.; Leung, L. R.; Liao, K.-J.; Lin, J.-T.; Lynn, B. H.; Manomaiphiboon, K.; Mass, C.; McKenzie, D.; Mickley, L. J.; O'neill, S. M.; Nolte, C.; Pandis, S. N.; Racherla, P. N.; Rosenzweig, C.; Russell, A. G.; Salathé, E.; Steiner, A. L.; Tagaris, E.; Tao, Z.; Tonse, S.; Wiedinmyer, C.; Williams, A.; Winner, D. A.; Woo, J.-H.; Wu, S.; Wuebbles, D. J. A Preliminary Synthesis of Modeled Climate Change Impacts on U.S. Regional Ozone Concentrations. *Bull. Amer. Meteor. Soc.* **2009**, *90* (12), 1843–1864. https://doi.org/10.1175/2009BAMS2568.1.

406 (24) Gong, X.; Kaulfus, A.; Nair, U.; Jaffe, D. A. Quantifying O_3 Impacts in Urban Areas Due
407 to Wildfires Using a Generalized Additive Model. *Environ. Sci. Technol.* **2017**, *51* (22), 13216–
408 13223. https://doi.org/10.1021/acs.est.7b03130.

409 (25) Mass, C. F.; Albright, M.; Ovens, D.; Steed, R.; Maciver, M.; Grimit, E.; Eckel, T.; Lamb,
410 B.; Vaughan, J.; Westrick, K.; Storck, P.; Colman, B.; Hill, C.; Maykut, N.; Gilroy, M.; Ferguson,
411 S. A.; Yetter, J.; Sierchio, J. M.; Bowman, C.; Stender, R.; Wilson, R.; Brown, W. Regional
412 Environmental Prediction Over the Pacific Northwest. *Bull. Amer. Meteor. Soc.* **2003**, *84* (10),
413 1353–1366. https://doi.org/10.1175/BAMS-84-10-1353.

414 (26) Pacific Northwest Environmental Forecasts and Observations
415 https://a.atmos.washington.edu/mm5rt/ (accessed Mar 6, 2020).

416 (27) Haixiang, G.; Yijing, L.; Shang, J.; Mingyun, G.; Yuanyue, H.; Bing, G. Learning from
417 Class-Imbalanced Data: Review of Methods and Applications. *Expert Systems with Applications*
418 **2017**, *73*, 220–239. https://doi.org/10.1016/j.eswa.2016.12.035.

419 (28) Jiang, N.; Riley, M. L. Exploring the Utility of the Random Forest Method for Forecasting
420 Ozone Pollution in SYDNEY. **2015**, *1* (5), 10.

421 (29) Ukkonen, P.; Manzato, A.; Mäkelä, A. Evaluation of Thunderstorm Predictors for Finland
422 Using Reanalyses and Neural Networks. *J. Appl. Meteor. Climatol.* **2017**, *56* (8), 2335–2352.
423 https://doi.org/10.1175/JAMC-D-16-0361.1.

424 (30) Jolliffe, I. T.; Stephenson, D. B. *Forecast Verification: A Practitioner's Guide in*
425 *Atmospheric Science*; John Wiley & Sons, 2012.

(31) Wilks, D. S. *Statistical Methods in the Atmospheric Sciences*; Academic press, 2011; Vol. 100.

(32) Doswell III, C. A.; Davies-Jones, R.; Keller, D. L. On Summary Measures of Skill in Rare Event Forecasting Based on Contingency Tables. *Weather and Forecasting* **1990**, *5* (4), 576–585.

(33) Murphy, K. P. *Machine Learning: A Probabilistic Perspective*; MIT press, 2012.

(34) Raschka, S. Model Evaluation, Model Selection, and Algorithm Selection in Machine Learning. *arXiv:1811.12808 [cs, stat]* **2018**.

(35) Falessi, D.; Narayana, L.; Thai, J. F.; Turhan, B. Preserving Order of Data When Validating Defect Prediction Models. 20.